OPEN ACCESS

European Journal of Engineering Science and Technology
ISSN 2538-9181

The Effect of Wire Rope Material on Vibration Characteristics

Hüseyin Dal[1*] and Murat Baklacı[2]

[1] Department of Mechanical Engineering, Engineering Faculty, Sakarya University, Sakarya, Turkey
[2] Department of Mechanical Engineering, National Defence University, Ankara, Turkey

ARTICLE INFO

Keywords:
Wire rope vibration isolator
Vibration isolation
Damping ratio

ABSTRACT

Wire rope vibration isolators (WRI) are used to protect particularly sensitive and high technology products from severe dynamic loads such as shock and vibration. WRI is widely used in many industries, especially in the defense and space industry. In this study, the effect of rope material used in WRIs on vibration characteristics was experimentally investigated. WRIs were fabricated using nuflex, stainless steel and galvanized steel ropes as the main material component of the rope. Design and fabrication of 3 identical WRI models each with a rope diameter of 3 mm, namely Nufleks (NWRI), stainless (SWRI) and galvanized steel rope vibration isolator (GWRI), were performed. The produced WRI models were subjected to tensile-compression tests under different speed and pre-load conditions and then, force-displacement responses were obtained. In addition, dynamic vibration tests of WRI models were performed using the shaker system and accelerometers. As a result of the studies, it was observed that the rope material used in the WRIs significantly affected the vibration characteristics. When the quasi-static test results are examined, it is clearly understood that GWRI exhibits a more rigid characteristic compared to other models. At the same time, when the damping ratios obtained from hysteretic cycles are compared, it is clearly seen SWRI has the highest damping ratio. When the dynamic tests performed by shaker are examined, it is clearly seen that the isolator with the best vibration isolation characteristics is SWRI.

1. Introduction

Vibration isolators are widely used to protect sensitive machinery equipment, electronic devices, military tools and equipment from harmful shock and vibration effects. Vibration isolators can come in a variety of designs, forms and features. Over the past years, various equipment has been designed to isolate the structure from unwanted vibration energy and to reduce vibration. Unlike conventional steel spring and elastic wedges, one of these types of vibration isolators are steel rope vibration isolators (WRI). WRI is widely used in industrial applications due to their high performance in shock isolation and vibration isolation. The most common use of WRIs is to

* Corresponding Author E-Mail Address: hdal@sakarya.edu.tr

Cite this article as:
Dal, H., & Baklacı, M. (2021). The Effect of Wire Rope Material on Vibration Characteristics. *European Journal of Engineering Science and Technology, 4*(1): 15-26. https://doi.org/10.33422/ejest.v4i1.608

minimize the vibration and shock effects that occur during the transportation of military equipment. Protection of sensitive electronic equipment from environmental shock effects and vibration effects caused by earthquakes is a separate application area. At the same time, it is the most appropriate and economical method to protect from the harmful effects of vibration in systems exposed to such shock and vibration effects. WRIs consist of holders and ropes made of different materials. The final WRI is then obtained by fixing the ropes between two holders that are parallel to each other. A relative movement occurs during active operation between the bundles of wires forming the rope. Due to this relative motion, the WRIs exhibit a non-linear characteristic due to the friction that occurs between each wire. WRIs are widely used due to their high damping performance and affordable cost (Balaji, Moussa, et al., 2015; Balaji, Rahman, et al., 2015). Damping occurs with the effect of friction between the ropes and at the same time creates an energy dissipation in the system depending on the damping. Thus, some studies have been carried out on the use of ropes in vibration isolations due to their mechanical characteristics (Rashidi & Ziaei-Rad, 2017; Spizzuoco et al., 2016; Vaiana et al., 2017). Due to this complex structure, its dynamic behavior cannot be adequately analyzed. They have benefits such as low cost, resistance to thermal effects, high fatigue strength and resistance to shock effects, in addition to the mechanical damping characteristics of WRIs in three main directions. Alexandri et al. studied the effectiveness of WRIs for seismic protection in electronic devices. In their experimental studies, they found that the WRI is suitable for seismic vibrations (Alessandri et al., 2015). In order to predict the vibration response of WRIs and to use isolators more effectively, it is very important to accurately define the dynamic characteristics of WRIs under both static and dynamic loads. Tinker and Cutchins created a quasi-experimental model with variable cloumb friction and non-linear stiffness to model the dynamic characteristics of the helical wire-rope isolator. In their studies, they observed that energy dissipation increased due to the damping effect with increasing excitation amplitude for all frequency values (Tinker & Cutchins, 1992). While a modified Bouc-Wen model is used to explain asymmetric hysteresis curves in the vertical position, the general Bouc-Wen model was used in their study to explain the symmetrical hysteresis loops of the isolators in the case of horizontal loading (Bouc, 1971; Wen, 1976). As a result, it has been obtained from the study that the hysteresis damping of WRI decreases with the increase of the shaker excitation amplitude. However, the results were obtained by applying the limited displacement amount in horizontal and vertical directions to the WRI. Ko and Ni developed an experimental model to describe the hysteresis power of WRI (Ko et al., 1992). In their experimental study, it was observed that the force and displacement hysteresis cycles of WRI are independent of frequency but dependent on amplitude. Gerges developed a quasi-analytical model to describe the force displacement curve for a wire rope under tensile compressive loading, in which all model parameters are verified by the spring characteristics and dimensions (Gerges, 2008). Leenen and et al. have studied the non-linear hysteresis characteristics of a WRI under static harmonic cycle load (Leenen, 2002). In their work, a modified Bouc-Wen model was used to describe the force displacement hysteresis loops of the WRI. Schwanen and et al. studied a modified Bouc-Wen model to describe the hysteresis behavior of a WRI under quasi-static cycle load (Zhao et al., 2013). However, as a result of the studies, the dynamic behavior of WRI could not be predicted exactly. For large displacement amplitudes, acceptable results were obtained as a result of theoretical frequency sweep simulation. Paolacci and Giannini conducted studies on helical WRI for seismic protection in high voltage electrical equipment (Paolacci & Giannini, 2008). The efficiency of the isolation system is defined by simulating the seismic response of a 420 KV switch using a regulated Bouc-Wen model. Zhou and et al. studied an artificial neural network-based hybrid modeling technique to model the hysteresis behavior of a helical WRI (Chungui et al., 2009). Dynamic tests were carried out at two different amplitudes and frequencies. Experimentally obtained data were then used to develop a hybrid model for any system. However, the method requires more experimental

data to predict the dynamic behavior of the isolator at frequencies and amplitudes other than experimental studies. In their study, a closed shape approach is applied to the isolation system and then the response curves are obtained. Rashidi and Ziaei-Rad examined the dynamic characteristics of WRI. The experiments were carried out using both quasi static and dynamic tests. A modified Bouc-Wen model was then used to predict the dynamic behavior of the WRI. Using the experimentally obtained data, an artificial neural network model was created and used to predict experimental situations not used in network training. It has been revealed that the results obtained from the artificial neural network can well predict the hysteresis behavior of WRI. Finally, Foss examined a new technique to determine the damping characteristics of a helical WRI from force displacement hysteresis loops of the isolator applied quasi-static load cycle instead of directly measuring the dynamic behavior of the isolator (Foss, 2006). In the literature research, hysteresis behavior of WRI exposed to quasi-static cycle load has been widely examined. However, there are more than one parameter that affects these hysteresis behaviors of isolators. Many parameters such as rope material used in the isolator, rope geometry, rope diameter, rope winding number and direction affect the isolator to exhibit a non-linear behavior in its dynamic characteristics. In this study, the effect of the rope material used in the isolator on the characteristics of the isolator is examined. For experimental studies, three different WRIs in identical sizes with different rope materials, namely galvanized, nuflex and stainless, were produced. Hysteresis curves of WRIs were obtained with experimental studies at different displacements under quasi-static cycle load. After quasi-static tests, dynamic tests of WRI 'were carried out by an electrodynamic shaker system. As a result of dynamic tests, damping characteristics of each WRI have been obtained.

2. Materials and Methods

2.1. Types of WRI

Galvanized, stainless and nuflex rope materials were preferred for the production of WRI. These types of materials, which are widely used in the industrial areas, are preferred in various applications according to their properties. The material called galvanized is preferred especially for equipment operating in corrosive environments. Galvanized coating process is carried out using the hot dip method with a steel-based material. The resistance of the new material obtained in corrosive environments is increased. However, as a result of the coating process applied, capillary cracks occur in the coating depending on the texture structure of the material, and this situation negatively affects the fatigue strength of the material. Nufleks is a steel-based material. Nuflex ropes are the types of ropes that have a large number of bundles and the diameter of the wires forming the bundles is very small. Due to the large number of bundles, when they are subjected to loading compared to conventional ropes, their relative rotation on their axes is restricted. At the same time, since the diameters of the wires forming the bundles are very small, they tend to bend easily and show high elasticity. Finally, 316 stainless steel was preferred for stainless material, which is a material with high corrosion resistance. For these three materials used in the study, elemental analysis was carried out using Hitachi X-MET8000 Optimum device. The results obtained for galvanized, stainless and nuflex materials as a result of elemental analysis are presented in Table 1.

Each of the ropes supplied has a rope diameter of 3 mm. WRI models are 60 mm high and 43 mm wide, and all models have identical geometric dimensions. For experimental studies, 3 different WRI models were designed and produced: stainless (SWRI), nuflex (NWRI), and galvanized (GWRI).

Table 1.
Elemental analysis results for WRI rope materials

	SWRI	NWRI	GWRI
Cr	16.88±0.149	0.14±0.014	0.14±0.014
Ni	10.27±0.129	-	-
Mn	10.27±0.129	0.52±0.027	0.49±0.030
Mo	10.27±0.129	-	-
Si	10.27±0.129	1.57±0.068	1.60±0.078
Cu	10.27±0.129	0.04±0.008	0.04±0.008
Co	10.27±0.129	0.10±0.008	0.10±0.008
P	10.27±0.129	0.25±0.023	0.25±0.023
Fe	-	96.89±0.27	97.19±0.30
Zn	-	0.21±0.015	0.21±0.015
S	-	0.21±0.011	0.21±0.011
W	-	0.03±0.010	0.03±0.010

2.2. Fabrication of Models of SWRI, NWRI and GWRI

The production of 3 different SWRI, NWRI and GWRI models, all of which are identical in geometric dimensions, was carried out at the Sakarya University Mechanical Engineering Vibration Laboratory. Steel ropes prepared in equal lengths were fixed in the middle between two plates. Later, the ends of the idle ropes were twisted in 'S' shape and assembled between the other two plates on the opposite side. Finally, the final WRIs were obtained. The production stage and the final model produced are shown in Figure 1.

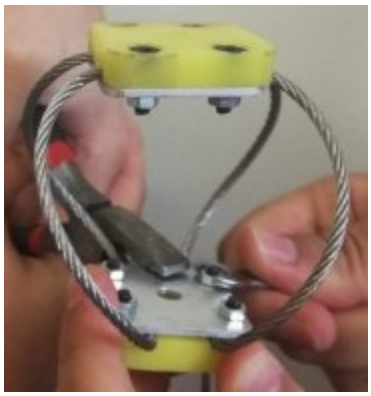

Figure 1. Assembly of WRI

2.3. Quasi-Static Tests

The quasi-static tests of all WRI models were carried out using the Instron brand test device at the Sakarya University Metallurgy and Materials Engineering Mechanical Stress Laboratory. Load-displacement tests were carried out at 3 different speeds, 10 mm/min, 50 mm/min and 100 mm/min for each model. Tensile and compression forces were applied to each WRI model from the accepted static equilibrium point by giving a certain preload Figure 2. Quasi-static hysteresis loops of each WRI model were obtained. Linear spring coefficients and damping ratios of each WRI model were determined by means of Hysteresis loops.

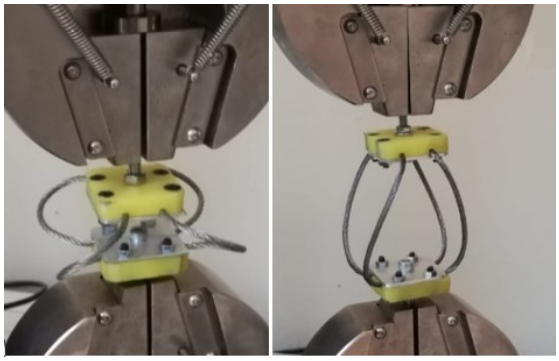

Figure 2. Quasi-static tests of WRI

The force-displacement response was obtained by applying a linear force to the WRIs from the equilibrium point as a full cyclic load. Some of the energy is absorbed while the WRI undergoes deformation. The amount of energy absorbed by the WRI during the deformation process represents the hysteresis amount of the WRI. The loading and unloading displacement curves in the force-displacement response are called the hysteresis loop as seen in Figure 6. During deformation, internal creep occurs between the contact surfaces of the rope wires of WRI and between the material molecules. Frictional resistance causes some energy loss during deformation when the WRI undergoes full cycle deformation. This energy loss is expressed by hysteresis, E_{diss}. The opposite of hysteresis is known as resilience. Resilience, on the other hand, refers to the amount of E_{sto} elastic energy stored in the WRI as a result of deformation and recovered when the loading is removed. E_{sto} also refers to the total amount of energy required to deform the WRI as seen Figure 3.

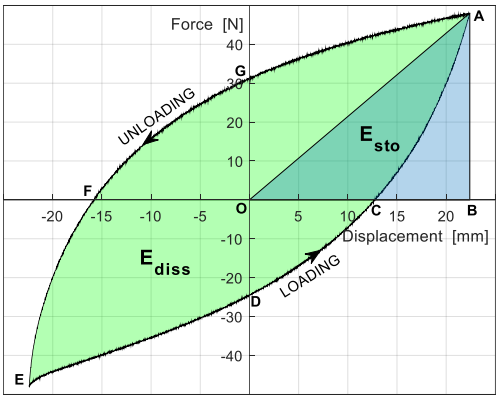

Figure 3. Experimental hysteresis curve of WRI for 10 mm/min speed

In Figure 6, the area covered with ACDEFG curves expresses the hysteresis amount of the WRI and the area of the ΔAOC triangle expresses the WRI resilience amount. The ratio between hysteresis and total energy is known as the damping ratio. The ratio of the actual damping factor to the critical damping factor is expressed as the damping ratio ξ. The damping ratio and spring coefficient of each WRI model can be obtained by means of hysteretic loops. The stiffness of each WRI model can be determined by the slope of the line segment OA that connects the O center point and the A end point of the closed loop that occurs during loading and unloading. The equivalent hysteretic damping of a nonlinear structural system for equivalent viscous damping can be expressed (Warburton, 1995). Similarly, damping ratio of WRI can be calculated with the help of E_{diss} and E_{sto} energies by using the following equation by using hysteresis loops (Bratosin & Sireteanu, 2002).

$$\xi_{loop} = \frac{1}{4\pi}\frac{E_{diss}}{E_{sto}} \tag{1}$$

2.4. Vibration Tests of WRI

Vibration tests with swept sine, harmonic and impulse methods were performed for WRI models using the shaker system in the Mechanical Engineering Vibration Laboratory of Sakarya University. WRIs were exposed to vibrations of different amplitudes in the frequency range of 0-100 Hz. Test data of WRI models were collected with accelerometers and data collection system. Natural frequencies, vibration isolation performances and damping ratios of the WRI models were obtained by vibration analysis. For vibration tests of WRIs, 300 N capacity LDS electrodynamic shaker, 4 channel Bruel & Kjaer brand Photon+ vibration analyzer (DAQ), 2 units of Bruel & Kjaer accelerometer with 100 mV/g sensitivity were used Figure 4. For preloading, 0.1 kg of mass is attached on the WRI models. One of the accelerometers is positioned on the shaker and the other on the WRI to measure the vibration of the WRI and evaluate the vibration isolation performance.

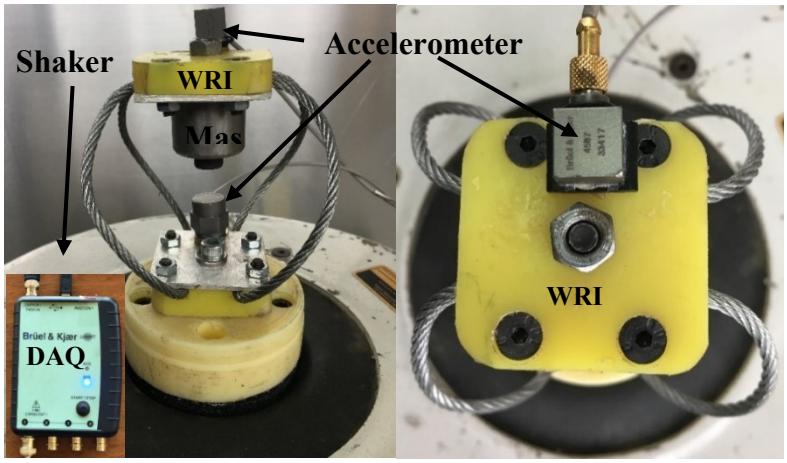

Figure 4. WRI test system, front view (left), top view (right)

In order to provide pre-stress to the isolators, a mass of 0.1 kg is attached to the WRI. The vertical frequency range (1-100 Hz) of the WRI models was determined by driving the jarring swept-sine function. The frequency response was obtained by collecting the dynamic behavior data of each model with accelerometers through vibration tests. During the test, the natural frequencies of WRIs were determined by observing and measuring the WRI behavior at each frequency. Vibration isolation performances of WRI models were examined by means of harmonic vibration test method using a vibration shaker. Impulse method was used to determine the damping ratio of WRI models with vibration test. While the WRI models subjected to harmonic load in a continuous regime state were vibrating, transient responses were obtained by suddenly interrupting the shaker excitation force. The damping ratios of each WRI model in the resonance frequency were calculated by using the logarithmic decrement method through the temporary responses of the system obtained. In transient vibration responses, the logarithmic decrement amount is found by taking the logarithm of the ratio of two consecutive acceleration amplitudes.

$$\delta = \log \frac{a_n}{a_{n+1}} \tag{2}$$

Where a_n is any decreasing acceleration amplitude in free vibration response, a_{n+1} is the next consecutive acceleration amplitude. By using the logarithmic reduction amount, ξ damping ratio can be calculated with the following equation.

$$\xi_{vib} = \frac{1}{\sqrt{1 + (\frac{2\pi}{\delta})\text{^}2}} \tag{3}$$

3. Results and Discussion

3.1. Quasi-Static Test Results

Force-displacement tests were applied to WRIs at 3 different speeds and in vertical direction. Since inertia effects will increase at high speeds, it is obvious that dynamic behavior will also change. Tests have been carried out at low speeds in order to neglect inertia effects. The velocity values in the quasi static tests were applied as 10 mm/min, 50 mm/min and 100 mm/min. Hysteresis curves were obtained with a displacement of 22.5 mm for GWRI and NWRI models and 25 mm for SWRI model. Hysteresis loops showing the force-displacement responses obtained at various speed and loading conditions as a result of the quasi-static tests of the WRI models are given in Figure 5, Figure 6 and Figure 7. As can be seen from these figures, WRIs show non-linear viscoelastic behavior. When the hysteresis loops are examined, the quasi-static force-displacement behaviors of the WRI models are very close to each other. For that reason, it can be assumed that low velocities do not have much effect on the force-displacement behavior of WRI models. However, when the results in the literature are seen, the rigidities and damping ratios at high velocity values vary as a function of velocity [15]. Therefore, the stiffness and damping values change as the speed increases.

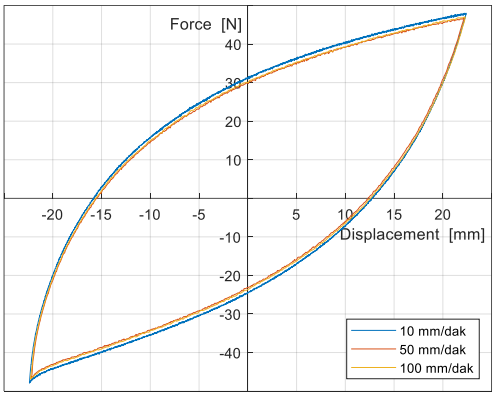

Figure 5. Hysteresis loops of GWRI for different speeds

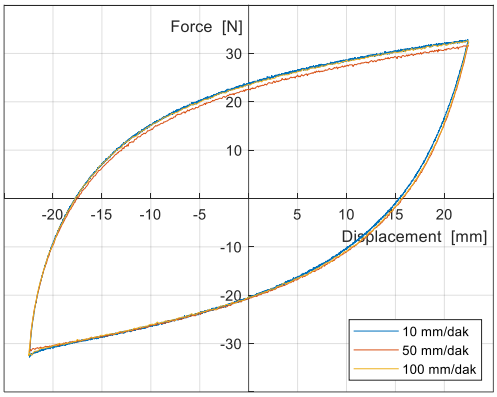

Figure 6. Hysteresis loops of NWRI for different speeds

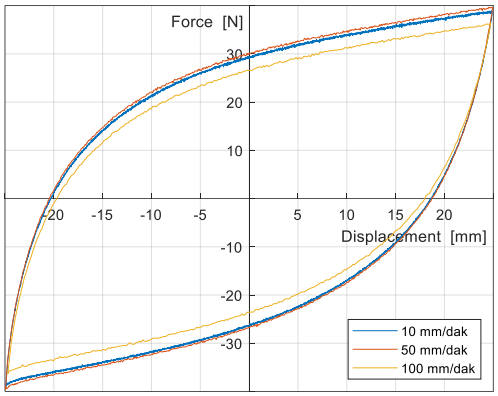

Figure 7. Hysteresis loops of SWRI for different speeds

Since hysteresis loops were assumed to unchanged at low speeds, only hysteresis loops with a speed of 100 mm/min of WRI models were examined. When Figure 8 is examined, it is clearly seen that the GWRI model behaves more rigidly at all speeds. The rigidity of the NWRI and SWRI models are closer to each other.

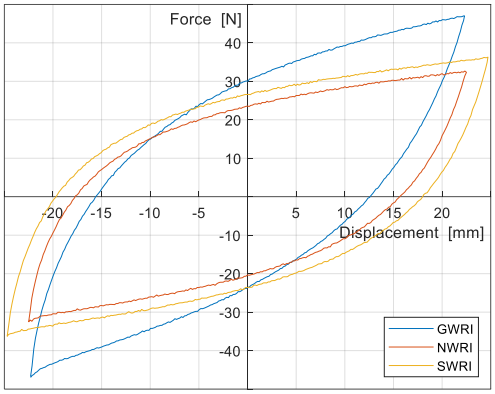

Figure 8. Hysteresis loops of WRI models for 100 mm/min

The stored and dissipated energies of each WRI model calculated using the hysteresis curves are given in Figure 9 and Figure 10, respectively. As can be seen from Figure 9 and Figure 10, the stored energy of the GRWI model is the highest and the dissipated energy of the SRWI model is the highest. Similarly, the stiffness of each WRI model can be calculated by using the hysteresis curves. Average stiffnesses of the WRI models are given in Figure 11. GWRI model has the highest stiffness with 2119.6222 N/m. The stiffness of the NWRI model was obtained as 1444.7655 N/m.

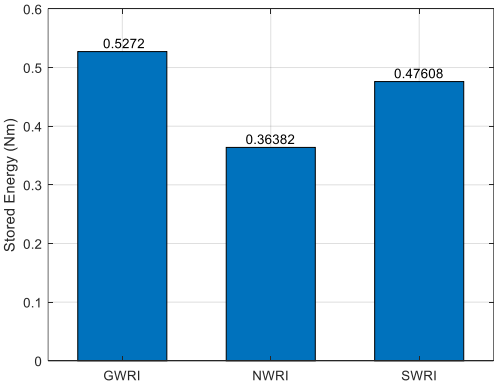

Figure 9. The average elastic stored energies of WRIs

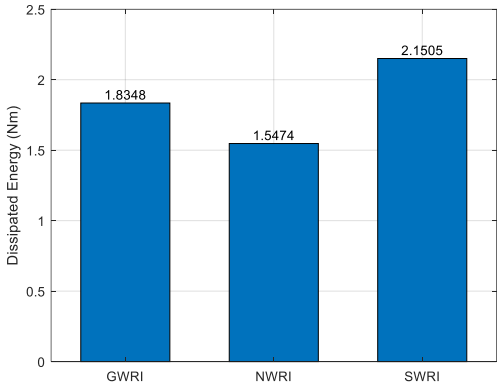

Figure 10. The average dissipated energies of WRIs

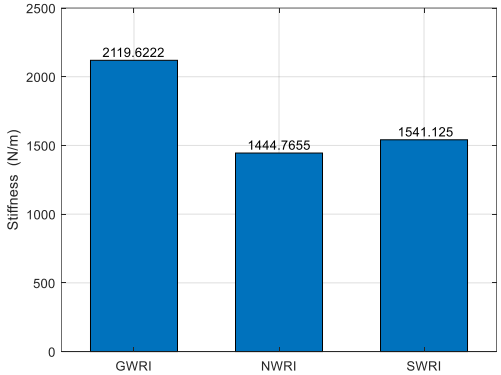

Figure 11. The average Secant stiffness of WRIs

By substituting the calculated stored and dissipated energy values in Equation 1, damping ratios of WRIs can be found, Figure 12. As seen in Figure 12, the damping ratio of the GWRI model is the lowest and the damping ratio of the SWRI model is the highest. According to these results, it can be concluded that the best WRI model for vibration isolation is SRWI and the worst model is GWRI.

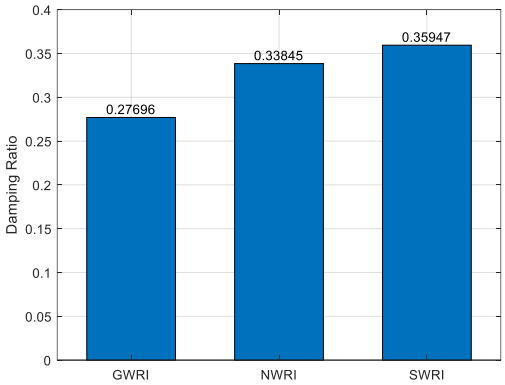

Figure 12. The average damping ratios of WRIs

3.2. Vibration Test Results

The acceleration-time response image of the NWRI model at 50 Hz excitation frequency is given in Figure 13. It is understood that the NWRI model provides very good vibration isolation at a frequency of 50 Hz. Because only a small part of the shocking acceleration affects NWRI, the rest is completely isolated by NWRI. Acceleration-time responses of other WRI models at 50 Hz are similar.

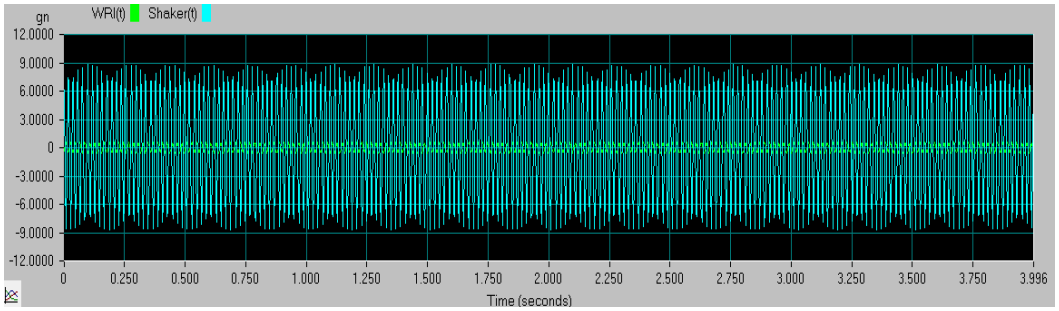

Figure 13. Acceleration-time response of the NWRI for 50 Hz

Transient vibration response of GWRI is shown in Figure 14. WRI damping parameters, ξ and natural frequencies, f_n obtained from vibration tests are given in Table 2. According to the vertical results obtained, the damping rate of the SWRI model is the highest and the damping rate of the GWRI model is the lowest. The damping rate results also confirm their vibration isolation performance.

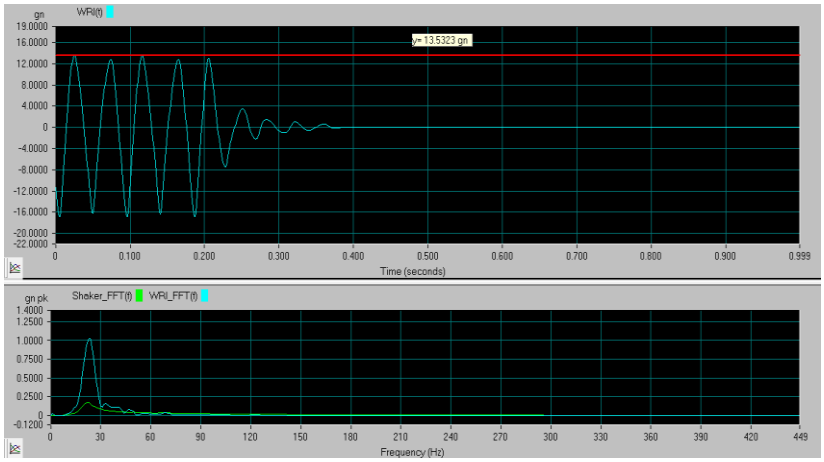

Figure 14. Transient vibration response of GWRI

Table 2.
Damping parameters obtained from the vibration test

	GWRI	NWRI	SWRI
ξ	0.18	0.21	0.26
$f_n\ [Hz]$	22	15	17

The damping rates obtained from the hysterical cycle and the damping rates obtained from the vibration test are compared in Figure 15. When the graph is examined, the damping ratio values obtained from the hysteresis curves are higher than the damping ratio values obtained from the vibration test. However, as can be seen from the graph, the damping values of WRIs increase proportionally for both test cases. This variability in the damping rates obtained from both tests is due to the velocity parameters applied in the tests. In quasi-static tests, not much variation is observed in the stiffness of WRI models for low speed values. For this reason, a comparison has been made for a fixed speed value of 100 mm/min for the quasi-static condition and vibration characteristics have been obtained. As can be understood from the quasi static tests, it has been observed that speed has a direct effect on vibration characteristics. The fact that the damping rates obtained from dynamic tests are smaller than those obtained from quasi-static tests are explained by the performance of dynamic tests at higher speeds.

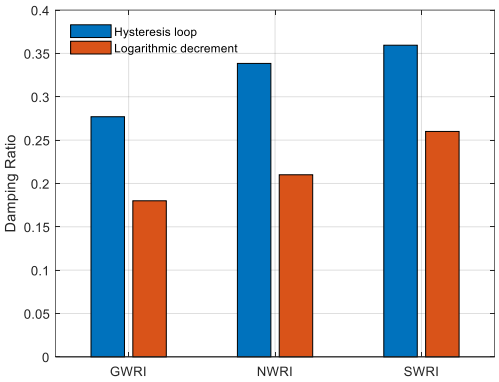

Figure 15. Comparison of WRI's damping ratios

4. Conclusions

Within the scope of the study, quasi-static and dynamic vibration tests of three different WRI models with different rope materials were carried out in order to examine how the rope material affects the vibration characteristics of WRI. Hysteresis curves of WRI models applying were obtained by applying the quasi-static tests at different speeds of 10, 50 and 100 mm/min. From the results of the hysteresis loops, the harmonic vibration test and logarithmic decrement method was seen that the GWRI model had the highest stiffness and the SWRI model had the highest damping. The other NWRI model was found to have moderate stiffness and damping ratios. The reason why the SWRI model exhibits higher damping characteristics is due to the higher friction characteristic, material including damping ability. Since the friction between wires, strands and core is minimum, GWRI model has high rigidity and low damping. Using the vibration shaker, the resonance frequencies of the GWRI, NWRI and SWRI models were found to be 22, 15 and 17 Hz, respectively. At the same time, vibration isolation performances were investigated all WRI models in the frequency range of 0 to 100 Hz. When the obtained vibration isolation performance graphs are examined, the models showing the best insulation characteristics at resonance frequency were determined as SWRI, NWRI and GWRI models, respectively. It has been observed that the rope material compositions of WRI models have a significant effect on the vibration characteristics of the vibration isolator.

References

Alessandri, S., Giannini, R., Paolacci, F., & Malena, M. (2015). Seismic retrofitting of an HV circuit breaker using base isolation with wire ropes. Part 1: Preliminary tests and analyses. *Engineering Structures*, *98*, 251–262. https://doi.org/10.1016/j.engstruct.2015.03.032

Balaji, P. S., Moussa, L., Rahman, M. E., & Vuia, L. T. (2015). Experimental investigation on the hysteresis behavior of the wire rope isolators. *Journal of Mechanical Science and Technology*, *29*(4), 1527–1536. https://doi.org/10.1007/s12206-015-0325-5

Balaji, P. S., Rahman, M. E., Moussa, L., & Lau, H. H. (2015). *Wire rope isolators for vibration isolation of equipment and structures-A review*. *78*, 12001. https://doi.org/10.1088/1757-899x/78/1/012001

Bouc, R. (1971). A Mathematical Model for Hysteresis. In *Acta Acustica united with Acustica* (Vol. 24, Issue 1, pp. 16–25).

Bratosin, D., & Sireteanu, T. (2002). Hysteretic damping modeling by nonlinear Kelvin-Voigt model. *Proceedings of the Romanian Academy*, *3*.

Chungui, Z., Xinong, Z., Shilin, X., Tong, Z., & Changchun, Z. (2009). Hybrid modeling of wire cable vibration isolation system through neural network. *Mathematics and Computers in Simulation*, *79*(10), 3160–3173. https://doi.org/10.1016/j.matcom.2009.03.007

Foss, G. C. (2006). Modal damping estimates from static load-deflection curves. *The Shock and Vibration Digest*, *38*, 535.

Gerges, R. R. (2008). Model for the Force-Displacement Relationship of Wire Rope Springs. *Journal of Aerospace Engineering*, *21*, 1–9. https://doi.org/10.1061/(ASCE)0893-1321(2008)21:1(1)

Ko, J. M., Ni, Y., & Tian, Q. L. (1992). Hysteretic behavior and empirical modeling of a wire-cable vibration isolator. *The International Journal of Analytical and Experimental Modal Analysis*, *7*(2), 111–127.

Leenen, R. (2002). *The modelling and identification of an hysteretic system: the wire as a nonlinear shock vibration isolator*. Technische Universiteit Eindhoven.

Paolacci, F., & Giannini, R. (2008). *Study of the effectiveness of steel cable dampers for the seismic protection of electrical equipment*.

Rashidi, S., & Ziaei-Rad, S. (2017). Experimental and numerical vibration analysis of wire rope isolators under quasi-static and dynamic loadings. *Engineering Structures*, *148*, 328–339. https://doi.org/10.1016/j.engstruct.2017.06.061

Spizzuoco, M., Quaglini, V., Calabrese, A., Serino, G., & Zambrano, C. (2016). Study of wire rope devices for improving the re-centering capability of base isolated buildings: Study of Wire Rope Devices for Improving the Re-Centering Capability. *Structural Control and Health Monitoring*, *24*. https://doi.org/10.1002/stc.1928

Tinker, M. L., & Cutchins, M. A. (1992). Damping phenomena in a wire rope vibration isolation system. *Journal of Sound and Vibration*, *157*(1), 7–18. https://doi.org/10.1016/0022-460X(92)90564-E

Vaiana, N., Spizzuoco, M., & Serino, G. (2017). Wire rope isolators for seismically base-isolated lightweight structures: Experimental characterization and mathematical modeling. *Engineering Structures*, *140*, 498–514. https://doi.org/10.1016/j.engstruct.2017.02.057

Warburton, G. B. (1995). Dynamics of structures, by Ray W. Clough and Joseph Penzien, 2nd edition, McGraw-Hill, New York, 1993. No. of pages: 738. ISBN 0-07-011394-7. *Earthquake Engineering \& Structural Dynamics*, *24*(3), 457–462. https://doi.org/10.1002/eqe.4290240311

Wen, Y.-K. (1976). Method for Random Vibration of Hysteretic Systems. *Journal of the Engineering Mechanics Division*, *102*(2), 249–263. https://doi.org/10.1061/JMCEA3.0002106

Zhao, Y., Wang, S., Zhou, J., Li, C., & Cheng, C. (2013). Modeling and identification of the dynamic behavior of stranded wire helical springs. *Journal of Vibroengineering*, *15*, 326–339.